Colloid & Polymer Science Colloid Polym Sci 272:820–829 (1994)

A turbidity study of particle interaction in latex suspensions

U. Apfel, R. Grunder, and M. Ballauff*

Polymer-Institut Universität Karlsruhe, Karlsruhe, FRG

Abstract: A turbidimetric analysis of particle interaction in latex suspensions is given. The turbidity measured at different wavelengths λ can be rendered by the product of an integrated form factor $Q(\lambda^2)$ and a suitably defined integrated structure factor $Z(\lambda^2, c)$. This factorization rests on the expansion of the form factor of the particles $P(q)$ and the structure factor $S(q)$ [$q = (4\pi/\lambda)\sin(\theta/2)$; θ: scattering angle] of the system in even powers of q. The accuracy of this approximation has been shown by calculating the turbidity for a system of hard spheres in terms of the Percus–Yevick structure factor by numerical integration. Also, the effect of polydispersity has been taken into account within the frame of Percus–Yevick–Vrij theory for non-uniform hard spheres. It is shown that the influence of small polydispersity (standard deviation below 8%) is within experimental uncertainty. The method is applied to precise UV-spectra ($400 \leq \lambda \leq 800$ nm) obtained from a polystyrene latex with a diameter of 77.4 nm. The integrated structure factor $Z(\lambda^2, c)$ obtained experimentally can be interpreted in terms of an effective diameter of interaction giving a measure for the strength of electrostatic interaction.

Key words: Turbidimetry – structure factor – light scattering – Percus–Yevick theory – latex

Introduction

In recent years there has been considerable progress in the understanding of structural properties of colloidal suspensions [1–3]. By the application of integral equation theories the radial distribution function $g(r)$ and the static structure factor $S(q)$ may be obtained and compared to the results of scattering experiments [2]. This comparison gives access to the interaction potential of the particles and allows the quantitative discussion of the factors governing colloidal stability. Polymeric latices as obtained by emulsion polymerization present very interesting systems for such studies since these particles can be prepared in a well-defined manner with a narrow size distribution [3]. Beside this, knowledge of particle interaction in polymer latex systems is of technical importance since it is intimately connected to the colloid stability and the flow behavior of these systems.

Up to now a considerable number of studies of the structure factor in polymer latices and of colloidal particles of comparable size has been performed [4]. If the diameter of the particles does not exceed certain limits, small-angle neutron scattering (SANS) [2, 4–7] or small-angle x-ray scattering (SAXS) [8–10] are suitable techniques. For sizes beyond 60 nm it becomes increasingly difficult to perform measurements at small values of the scattering vector q necessary to obtain full information on the structure factor $S(q)$. In particular, it is difficult to extrapolate $S(0)$ from these data with sufficient accuracy.

Light scattering [11–13] is suitable for the investigation of this range of q. On the other hand, measurements are restricted to the dilute regime because of the error introduced by multiple

---

* To whom all correspondence should be addressed

scattering at higher concentrations. As first shown by van Helden and Vrij [14] this problem can be alleviated by index matching which requires special solvent systems (cf. also ref. [15]). The contrast, however, will change with temperature. Therefore temperature-dependent studies are rendered very difficult and this method cannot be applied generally.

Turbidity is a technique which is practically insensitive to multiple scattering and is easy to perform. For a long time this method has been extensively used in dilute systems for determining the particle size in colloidal suspensions [16, 17]. Turbidimetric methods can also be used to extract thermodynamic data. Debye, Chu, and Woermann [18] were the first to investigate the critical opalescence of polymer solutions by this method. Turbidimetry has been applied repeatedly to the investigation of light scattering in the vicinity of the consolute point [19]. Vrij and coworkers [20–22] have pioneered the use of turbidity measurements for careful studies of particle interaction in sterically stabilized silica dispersions. These authors could demonstrate that turbidimetry leads to reliable parameters characterizing the interaction potential between the particles.

Extending the work of Vrij and coworkers [20–22], we discuss the evaluation of turbidimetric data to obtain information about the structure factor in the region of low angles. Special attention is paid to the effect of the size distribution of the particles. The theoretical deductions are compared to turbidity measurements of a polystyrene latex in water up to higher concentrations.

Theory

The turbidity τ is defined as the attenuation of a light beam by scattering when passing through a sample. Thus, $\tau = l^{-1} \ln(I_0/I_t)$ with I_0 being the incident intensity of the light, I_t the transmitted intensity, and l the length of the optical path. When absorption can be excluded the intensity of the scattered light and the turbidity are related through the following relation:

$$\tau = 2\pi \int_0^\pi R(q) \sin\theta d\theta \,, \qquad (1)$$

where $R(q)$ is the Rayleigh ratio for unpolarized light, $q = (4\pi n_0/\lambda_0)\sin(\theta/2)$ is the magnitude of the scattering vector, θ the scattering angle, n_0 the refractive index of the medium, and λ_0 the wavelength in vacuo. We assume that the size parameter $n_0\pi\sigma/\lambda_0$ with σ being the diameter of the particles is below unity. Therefore, it is permissible to use the Rayleigh–Debye (RD) theory (cf. reference [16], chapter 8) for the theoretical evaluation of the turbidity. Since the relative refractive index $m = n_p/n_0$, where n_p is the refractive index of the immersed particles, is considerably higher than 1, the Lorenz-Lorentz factor $(m^2 - 1)/(m^2 + 2)$ is not replaced by $(2/3)(m - 1)$ as is usually done within the RD approximation. Thus, the main error of the RD theory in this range of the size parameter $(n_0\pi\sigma/\lambda_0)$ is avoided and the RD expressions are expected to provide a very good approximation (cf. reference [16], p. 427).

A previous study of the polystyrene latex used herein by ultracentrifugation has shown that its size distribution is rather small and can be characterized by a standard deviation of ca. 6% [23]. From the model calculations for hard spheres displayed in reference [23] (cf. also the discussion of this point in reference [24]) it is clear that this small nonuniformity of particle size has a negligible influence on $S(q)$. It is well-known [12, 25, 26], however, that the nonuniformity has a profound influence on the small-angle region if the size distribution gets broader. Therefore, the extension of the treatment to non-uniform systems will be discussed also.

For particles with uniform size distribution the Rayleigh ratio $R(q)$ for a system of homogeneous spheres of diameter σ may be written as

$$R(q) = K^* c \cdot \left(\frac{n_0 \pi \sigma}{\lambda_0}\right)^3 \cdot P(q) \cdot S(q) \cdot (1 + \cos^2\theta) \,, \qquad (2)$$

where c denotes the mass concentration. The optical constant K^* is defined by

$$K^* = \frac{3n_0}{4\lambda_0 \rho_p} \left(\frac{m^2 - 1}{m^2 + 2}\right)^2 \qquad (3)$$

with ρ_p being the density of the particles. The form factor $P(q)$ accounts for the interference within the particles whereas the structure factor $S(q)$ is, as usual, related to the interparticular scattering.

In the region of low q and not too large particles, $P(q)$ can be approximated by

$$P(q) = 1 - \frac{1}{3}q^2R_g^2 + \frac{1}{25}q^4R_4^4 - \frac{4}{1575}q^6R_6^6\,, \quad (4)$$

where R_g^2 is the optical radius of gyration of the particle. The quantities R_4^4 and R_6^6 are suitably defined coefficients containing R_g^2 and the corresponding fourth and sixth moment. The structure factor is defined by [2]

$$S(q) = 1 + 4\pi\frac{N}{V}\int_0^\infty [g(r) - 1]\frac{\sin qr}{qr}r^2dr\,, \quad (5)$$

where N is the number of particles, V the volume and $g(r)$ the radial distribution function. It follows from Eq. (5) that in the region of small q, $S(q)$ may be expanded to yield

$$S(q) \simeq S(0) + \alpha q^2 - \beta q^4 + \gamma q^6 \quad (6)$$

Insertion of (4) and (6) into (2) and subsequent integration of Eq. (1) leads to:

$$\begin{aligned}\tau = K^*c\cdot\left(\frac{n_0\pi\sigma}{\lambda_0}\right)^3\frac{16\pi}{3}\Bigg[S(0) &+ 8\left(\frac{n_0\pi}{\lambda_0}\right)^2 \\ &\times\left(\alpha - S(0)\cdot\frac{1}{3}R_g^2\right) + \frac{448}{5}\cdot\left(\frac{n_0\pi}{\lambda_0}\right)^4 \\ &\times\left(S(0)\cdot\frac{1}{25}R_4^4 - \alpha\cdot\frac{1}{3}R_g^2 - \beta\right) \\ &+ \frac{5632}{5}\left(\frac{n_0\pi}{\lambda_0}\right)^6\left(-S(0)\frac{4}{1575}R_6^6\right. \\ &\left.+ \alpha\frac{1}{25}R_4^4 + \beta\frac{1}{3}R_g^2 + \gamma\right)\Bigg] + O(\lambda^8) \quad (7)\end{aligned}$$

This expression can be factorized (cf. also reference [22]) into a product of two functions $Q(\lambda^2)$ and $Z(\lambda^2, c)$:

$$\begin{aligned}Q(\lambda^2) = 1 &- \frac{8}{3}\left(\frac{n_0\pi}{\lambda_0}\right)^2R_g^2 + \frac{448}{125}\left(\frac{n_0\pi}{\lambda_0}\right)^4R_4^4 \\ &- \frac{22528}{7875}\left(\frac{n_0\pi}{\lambda_0}\right)^6R_6^6 + O(\lambda^8) \quad (8)\end{aligned}$$

and

$$\begin{aligned}Z(\lambda^2, c) = S(0) &+ 8\alpha\left(\frac{n_0\pi}{\lambda_0}\right)^2 \\ &- \frac{448}{5}\left[\beta + \frac{2}{21}\alpha\cdot R_g^2\right]\left(\frac{n_0\pi}{\lambda_0}\right)^4 \\ &+ \frac{512}{5}\left[11\gamma + \frac{4}{25}\alpha R_4^4 + \frac{4}{3}\beta R_g^2\right. \\ &\left.- \frac{2}{9}\alpha(R_g^2)^2\right]\left(\frac{n_0\pi}{\lambda_0}\right)^6 + O(\lambda^8) \quad (9)\end{aligned}$$

leading to

$$\tau = K^*c\cdot\left(\frac{n_0\pi\sigma}{\lambda_0}\right)^3\cdot\frac{16\pi}{3}\cdot Q(\lambda^2)\cdot Z(\lambda^2, c) \quad (10)$$

Thus, the turbidity may be factorized into two factors where $Q(\lambda^2)$ refers solely to the intraparticular interferences. Consequently, the function $Q(\lambda^2)$ may be termed "turbidity form factor". Despite the fact that the fourth and the sixth order terms in (9) still contain the radius of gyration of the particles and R_4^4, the quantity $Z(\lambda^2, c)$ still can be regarded as a "turbidity structure factor". It has to be noted that Eq. (10) may be also considered as the definition of $Z(\lambda^2, c)$ since the factorization Eq. (10) can be extended to an arbitrary order in λ^2.

Given the validity of Eq. (10) the evaluation of the turbidity data can therefore be done in the usual manner by separate extrapolations of $c \rightarrow 0$ and $\lambda^{-2} \rightarrow 0$. Hence, (cf. also ref. [22]):

$$\left(\frac{\tau}{c}\right)_{c=0} = K^*\left(\frac{n_0\pi\sigma}{\lambda_0}\right)^3\frac{16\pi}{3}Q(\lambda^2) \quad (11)$$

$Z(\lambda^2, c)$ as defined by Eq. (9) can be obtained from the experimental turbidities by

$$Z(\lambda^2, c) = \frac{\left(\frac{\tau}{c}\right)}{\left(\frac{\tau}{c}\right)_{c=0}} \quad (12)$$

Equations (10) and (11) suggest that $Q(\lambda^2)$ for a given wavelength can be obtained by extrapolation of τ/c to vanishing concentration. Division of τ/c obtained from finite concentrations by the intercept of this plot then leads to $Z(\lambda^2, c)$. The parameters S(0), α, β and γ in $Z(\lambda^2, c)$ (Eq. (9)) can be obtained by a respective fit of Eq. (9) to experimental data.

Following Vrij and coworkers [22] the above considerations can be easily extended to systems with finite size distribution. Thus a "measured integrated structure factor" $Z_M(\lambda^2, c)$ can be defined by

$$Z_M(\lambda^2, c) = \frac{\int_0^\pi \bar{P}(q) \cdot \bar{S}(q)(1 + \cos^2\theta)\sin(\theta) d\theta}{\int_0^\pi \bar{P}(q)(1 + \cos^2\theta)\sin(\theta) d\theta}\,, \quad (13)$$

where $\bar{P}(q)$ and $\bar{S}(q)$ are suitable averages (see Eqs. (26) and (28), respectively, of ref. [22]) of the form factor and the structure factor, taken over the size distribution.

In the limit of very small concentrations $Z(\lambda^2, c)$ as well as $Z_M(\lambda^2, c)$ may be rendered approximately by:

$$Z(\lambda^2, c)^{-1} \approx 1 + 2B_{\mathrm{app}} c\,, \quad (14)$$

where the apparent second virial coefficient B_{app} is depending on wavelength [20–22]. Thus, Eq. (14) suggests that plots of the reciprocal specific turbidity versus concentration in the dilute regime can be used to extrapolate the specific turbidity at infinite dilution.

Model calculations

For a detailed study of the turbidity structure factor (Eq. (9)) it is expedient to use a system of hard spheres as a starting point. For hard spheres the structure factor $S(q)$ may be calculated analytically [27] in the frame of the Percus–Yevick theory [28]. Vrij [29] has shown that an analytical solution can be obtained for the polydisperse case, too. We first discuss the case of monodisperse hard spheres where the approximative expression (7) can be compared to the result obtained from a numerical integration of Eq. (1). For the latter calculation the exact form factor of monodisperse hard spheres and the analytical expression of the Percus–Yevick structure factor [27] has been employed. Thus, the range of validity of Eqs. (7) to (9) can be assessed directly. In a second step these results are compared to the "measured integrated structure factor" $Z_M(\lambda^2, c)$ as obtained by numerical integration (cf. Eq. (13)) of Vrij's structure factor [29] on non-uniform systems.

For a system of monodisperse hard spheres series expansion [14, 30, 31] leads to the following expressions for $S(0)$ [28] and the coefficients α [14], β [31], and γ:

$$S(0) = \frac{(1 - \phi)^4}{(1 + 2\phi)^2} \quad (15)$$

$$\alpha = \frac{\phi d^2 (16 - 11\phi + 4\phi^2)(1 - \phi)^4}{20(1 + 2\phi)^4} \quad (16)$$

$$\beta = \phi d^4 \frac{(80 - 72\phi + 12\phi^2 + 7\phi^3)(1 - \phi)^4}{2800(1 + 2\phi)^4} - \frac{\alpha^2}{S(0)} \quad (17)$$

$$\gamma = \phi d^6 \frac{(40 - 41\phi + 4\phi^2 + 6\phi^3)(1 - \phi)^4}{75600(1 + 2\phi)^4} - 2\alpha\phi d^4 \frac{80 - 72\phi + 12\phi^2 + 7\phi^3}{2800(1 + 2\phi)^2} + \frac{\alpha^3}{S(0)^2}\,, \quad (18)$$

with $\phi = (N/V)(\pi/6)d^3$ being the volume fraction of the hard spheres in the system and d the effective diameter of the spheres. For hard spheres d is equal to the diameter of the spheres σ. It may assume higher values when modeling the electrostatic interaction (see below).

First, from a comparison of the turbidity at vanishing concentration calculated numerically and by resorting to Eq. (8) it can be concluded that expression (8) is indeed a very good approximation for spheres up to 120 nm and the range of wavelength typically used in a turbidimetric experiment (400–800 nm). In a next step the accuracy of Eq. (9) as compared to the exact result obtained by numerical integration may be done. This comparison is shown in Fig. 1a for different volume fractions.

Here, a plot of the exact $Z(\lambda^2, c)$ (obtained from numerical integration of Eq. (1)) is displayed together with the result from the approximation Eq. (9) together with (14) to (18). The calculation was done for monodisperse hard spheres of diameter 120 nm dispersed in water. The dependence of the refractive index on wavelength was calculated using the relation by Maron et al. [32] ($n^2 = 1.7521 + 8110/\lambda_0^2$; λ_0 in nm). The factorization Eq. (10) together with (8) and (9) provides a very good description of the turbidity structure factor for spheres with diameter 120 nm above wavelengths of 500 nm; for smaller diameters even full

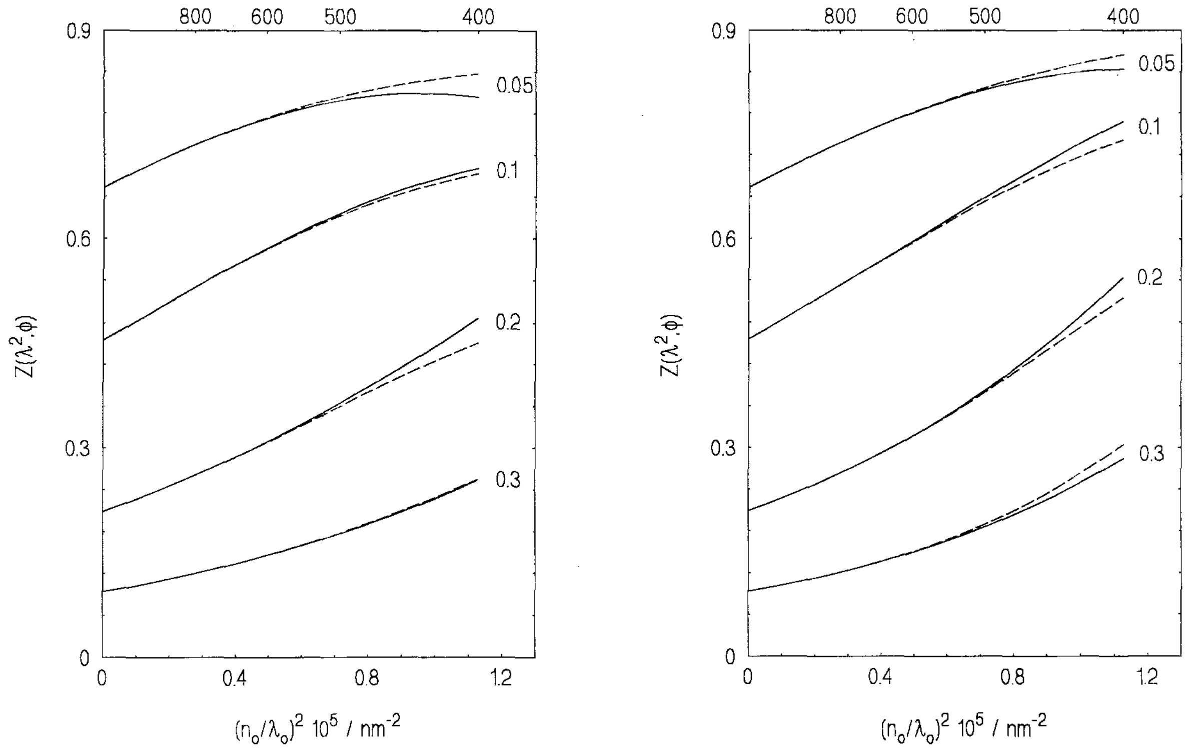

Fig. 1. a: Integrated structure factor $Z(\lambda^2,c)$ (cf. Eq. (10)) calculated for a system of monodisperse hard spheres with 120 nm diameter using the Percus–Yevick structure factor [27, 28]. The solid line refers to the approximation Eq. (9); the dashed lines to the exact result calculated by numerical integration of Eq. (1) and division by $(\tau/c)_0$ according to Eq. (12). The numbers in the graph are the respective volume fractions; the figures above the graph indicate the respective wavelength. b: Integrated structure factor $Z(\lambda^2,c)$ (cf. Eq. (10)) calculated for a system of monodisperse hard spheres with 80 nm diameter but an effective diameter d of interaction of 120 nm (see text for explanation). The solid line refers to the approximation Eq. (9); the dashed lines to the exact result calculated by numerical integration of Eq. (1) using the Percus–Yevick structure factor [27, 28] and subsequent division by $(\tau/c)_0$ (Eq. (12)). The numbers in the graph are the respective volume fractions; the figures above the graph indicate the respective wavelength

agreement over the entire range of accessible wavelengths can be demonstrated. In particular, the agreement improves with increasing volume fraction of the spheres due to the decrease of the coefficients α, β, and γ. Therefore it can be concluded that the expansions (4) and (6) are fully applicable for the problem under consideration here.

If the particles are highly charged their interaction is well described by the repulsive part of the DLVO potential [1, 2]. In first approximation the magnitude of the repulsion may be modeled in terms of an effective diameter d which exceeds the actual diameter σ of the spheres ([2, 33]; see below for further discussion of this point). Again, by a comparison of the result of the numerical integration of Eq. (1) with the approximation (10) (see Fig. 1b) it becomes evident that the effective diameter d determines the range of wavelengths where $Z(\lambda^2, c)$ can be calculated by resorting to Eq. (9). Here, too, Eq. (9) provides a good description for wavelengths above 500 nm. Since the effective diameters obtained from the experimental data discussed herein are considerably smaller, it is concluded that Eq. (9) is justified for the whole range of accessible wavelengths.

It has been concluded (cf. reference [31] and further references cited there) that the van der Waals attraction between the particles necessitates the inclusion of a q^3-term in the expansion Eq. (6). In principle, such a term can be added to the theory by suitable alteration of Eq. (9). Trial calculations for the system polystyrene/water under consideration here (see below) showed,

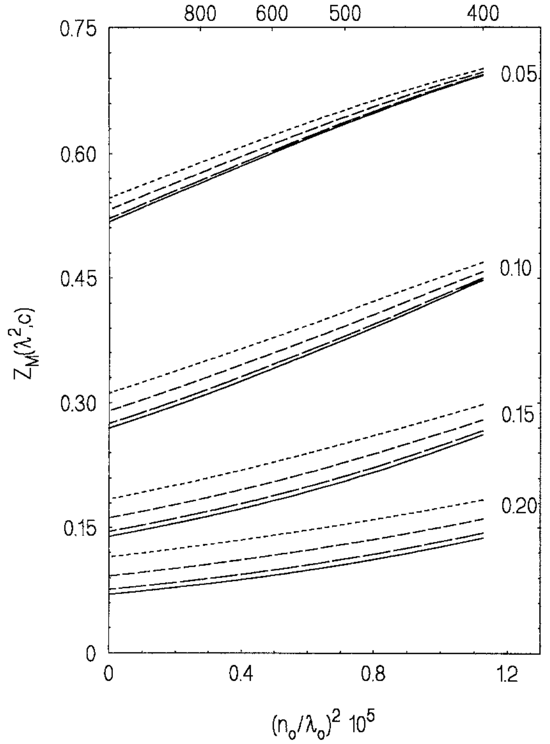

Fig. 2. "Measured integrated structure factor" $Z_M(\lambda^2,c)$ calculated according to Eq. (13) for a system of polydisperse hard spheres having a Gaussian size distribution. In all cases the z-average diameter of the spheres was 80 nm. The solid line refers to the monodisperse case; for the other curves the standard deviations are as follows: — —: 7.5%, - - - -: 15%, ... : 22%

however, that this term has only a small influence and the influence of van der Waals attraction between the particles may be treated as a perturbation.

In order to include the effect of nonuniformity $Z_M(\lambda^2, c)$ is evaluated for a system of hard spheres with Gaussian size distribution by numerical integration of Eq. (13). Figure 2 displays the result for four different standard deviations.

In all cases the z-average diameter of the hard spheres has been kept constant and amounts to 80 nm. As already evident from earlier discussions [24] of this problem, non-uniformity is nearly negligible for standard deviations below ca. 8%. Broader size distributions, however, will result in an increase of $Z_M(\lambda^2, c)$, in particular at higher volume fractions. The effect is most pronounced near $q = 0$, i.e., for increasing wavelength. These findings are in accord with previous discussions and deductions [24–26], of course.

Experimental

The polystyrene latex used herein had a very narrow size distribution and was prepared as described recently [23]. The number- and the weight-average diameter were determined by ultracentrifugation ($\sigma_n = 68.9$ nm; $\sigma_w = 71.1$ nm). The stock latex was dialyzed exhaustively against 10^{-2}M KCl solution to adjust the ionic strength to approximately 10^{-2}. After filtration through a 1,2 μm filter (Millipore) the stock latex was diluted using 10^{-2}M KCl solution.

Measurements of the extinction between 400 and 800 nm have been conducted using a Perkin–Elmer Lambda-3 spectrometer thermostatted at 25 °C. Since the front factor of Eq. (7) varies as λ^{-4} the measurements were done using different lengths of the optical path (0.1–5 cm) depending on wavelength. Only data deriving from transmissions between 0.03 and 0.95 were found to be accurate enough. In all cases the turbidity was found independent of the length of the optical path within given limits of error (cf. the discussion of this point in ref. [20]). From the strict validity of the Lambert-Beer law it is evident that the determination of τ is not afflicted by multiple scattering or forward scattering.

The density of the polystyrene particles in suspension was determined using a DMA 60 apparatus supplied by Paar (Graz, Austria). The value found herein (1.055g/cm^3) is in good agreement with the one supplied by literature (1.054g/cm^3, [17]).

Results and Discussion

As discussed above the theoretical deductions suggests that the specific turbidity τ/c will decrease markedly due to interparticular interaction. The experimental values of τ/c as function of c corroborate this analysis (see Fig. 3a). In the region of low c (Fig. 3b) the reciprocal specific turbidity is linear with respect to c as expected from Eq. (14). Therefore, this plot is appropriate for the extrapolation of τ/c to vanishing concentration.

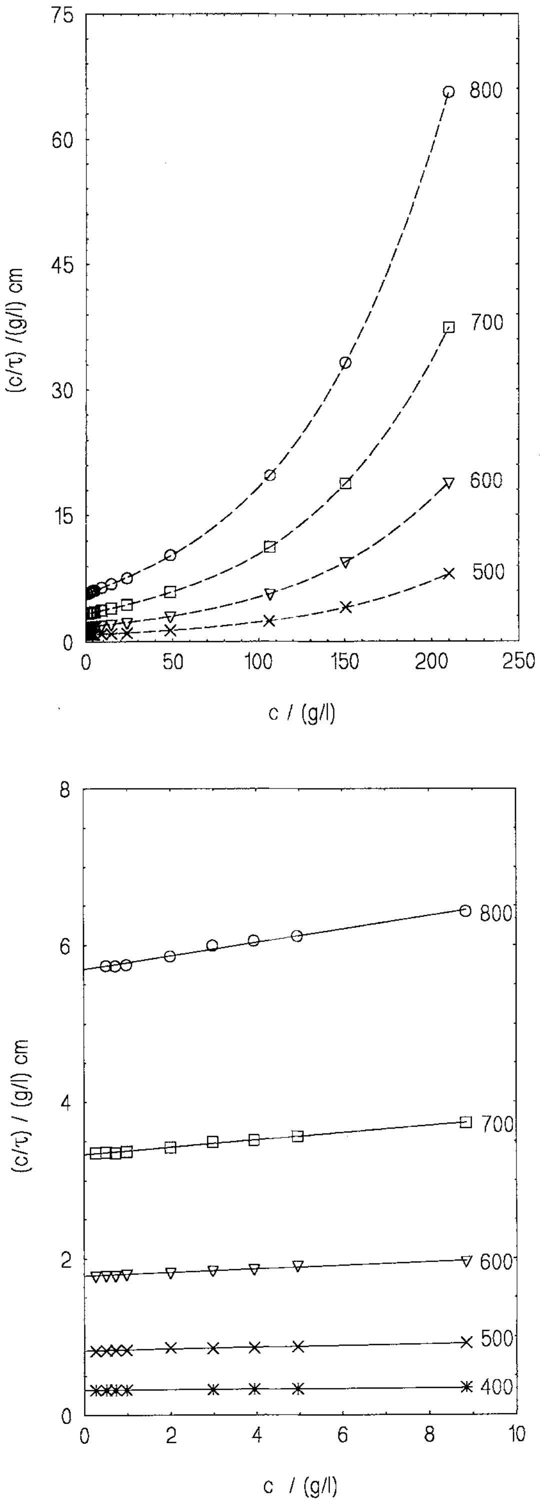

Fig. 3a,b. Plots of the reciprocal specific turbidity c/τ obtained experimentally from the polystyrene latex as function of concentration. 3b: dilute regime. The numbers indicated in the graph refer to the respective wavelengths in nm

From the specific turbidities $(\tau/c)_0$ obtained from the intercepts of Fig. 3b the integrated form factor $Q(\lambda^2)$ can be obtained through Eq. (11). For this evaluation the dependence of the refractive indices on wavelength must be known. For water the relation by Maron et al. [31] (see above) has been used; the respective relation for polystyrene ($n^2 = 2.4251 + 36054/\lambda_0^2$; λ_0 in nm) was constructed using the data compiled by Devon and Rudin [34]. Figure 4 displays the resulting $Q(\lambda^2)$ as function of λ^2. The solid line refers to a fit of Eq. (8) to the experimental data assuming a homogeneous sphere with 77.4 nm. The latter figure compares favorably with the value of 71.1 nm obtained by ultracentrifugation. Within experimental uncertainty Eq. (8) provides a good description of the data, especially when considering the error of the refractive index of water and polystyrene at higher wavelength. Thus, a small change of the parameters in the Cauchy-relation for polystyrene ($n^2 = 2.4418 + 2.4668 \cdot 10^4/\lambda^2 + 1.6291 \cdot 10^9/\lambda^4$; λ in nm) leads to full agreement of theory and experiment; the deviations seen in Fig. 4 are therefore due to finite accuracy of the refractive index of polystyrene.

It is therefore evident that the extrapolation of the reduced turbidity as shown in Fig. 3b leads to consistent values for the integrated form factor $Q(\lambda^2)$. Even in absence of a reliable dispersion

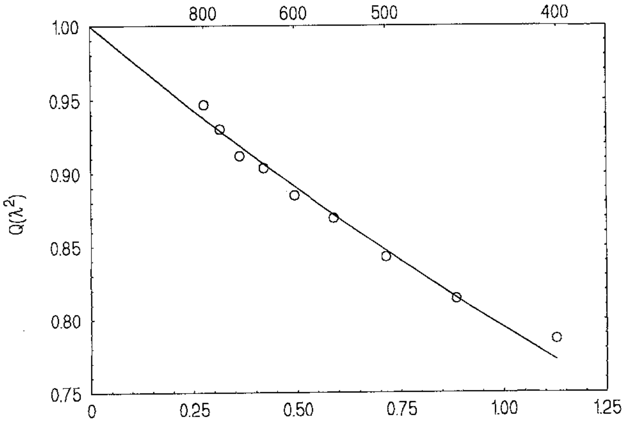

Fig. 4. Turbidity form factor $Q(\lambda^2)$ (Eq. (8)) obtained by the reduced turbidity at vanishing concentration. The solid line gives the fit of the theoretical expression Eq. (8) leading to a diameter σ of 77.4 nm

relation of the latex polymer the subsequent evaluation of the integrated structure factor $Z(\lambda^2,c)$ can be done without difficulty. This is evident from Eq. (12) together with (11) and (10) showing that the experimental values of $(\tau/c)_0$ are sufficient for calculating $Z(\lambda^2,c)$; i.e., the explicit evaluation of $Q(\lambda^2)$ is not necessary.

To assess possible errors due to polydispersity, calculations of $Q(\lambda^2)$ using the experimental size distribution have been performed. As already discussed above, the small standard deviation of the latex under consideration here leads to nearly negligible alterations of the parameters which are well below experimental uncertainty. Therefore, the influence of polydispersity can be safely dismissed in the following comparison of theory and experiment.

Having discussed the dilute regime we now turn to the integrated structure factor $Z(\lambda^2,c)$ as obtained by application of Eq. (12) to the reduced turbidities at higher concentrations. The resulting data are displayed in Fig. 5.

The analysis of $Z(\lambda^2,c)$ can be done as follows: The accuracy of $Z(\lambda^2,c)$ as function of λ^2 and volume fraction and the range of wavelength is not sufficient to determine $S(0)$ and all expansion coefficients independently. Therefore, the strength of the electrostatic repulsion will be discussed in terms of an effective diameter of interaction. This can be achieved as follows (see, e.g., ref. [28, 33, and 35]): The repulsive interaction of the latex spheres may be treated in terms of the Weeks, Chandler, and Anderson (WCA) perturbation theory [36, 28]). This can be argued from the fact that at the rather high ionic strength the electrostatic repulsion between the particles is quite steep (see, e.g., Goodwin et al. [33]). Thus the structure factor $S(q)$ can be separated into two parts

$$S(q) = S_{\mathrm{hs}}(q) + \frac{N}{V}\cdot B(q)\,, \tag{19}$$

where $S_{\mathrm{hs}}(q)$ is the structure factor of the hard sphere reference fluid and $B(q)$ is the "Blip-function" given by

$$B(q) = 4\pi\int_0^\infty dr\, r^2 y(r)\,[\exp(-V(r)/kT) - \exp(-V_{\mathrm{hs}}(r)/kT)]\,\frac{\sin(qr)}{qr}\,. \tag{20}$$

Here, $V_{\mathrm{hs}}(r)$ is the hard-sphere potential, $V(r)$ the steep potential of the latex spheres, and $y(r)$ is defined by

$$y(r) = g_{\mathrm{hs}}(r)\exp(V_{\mathrm{hs}}(r)/kT)\,, \tag{21}$$

with $g_{\mathrm{hs}}(r)$ being the pair correlation function of the hard sphere reference fluid. Within the WCA approach the effective diameter d of the hard sphere reference fluid is chosen by the condition $B(0) = 0$ such that $S(0) = S_{\mathrm{hs}}(0)$ (cf. [28, 35, 36]). Therefore, the effective volume fraction ϕ_{eff} follows directly from the $S(0)$ values determined experimentally. The effective volume fraction then allows the evaluation of the effective diameter d of interaction. In order to check the validity of this procedure when dealing with electrostatic repulsion, model calculations have been performed using the RMSA structure factor [37, 38]. Thus, $S(q)$ has been calculated for spheres of 80 nm diameter and a typical effective surface charge of the order of $500e^-$ per sphere (cf. ref. [39]). The ionic strength was chosen to 10^{-2}M. For the q-range explored by the turbidimetric experiment the structure factor calculated for hard spheres coincides with the RMSA result when the effective diameter d is chosen by the condition $B(0) = 0$. For lower ionic strength and higher values of q, however, differences become appreciable and the perturbative approach should not be used anymore. Nevertheless, for the present experimental data a description in terms of an effective diameter d of interaction should be reasonable.

The solid lines in Figs. 5a and b show the fit of the monodisperse hard sphere $Z(\lambda^2,c)$ (Eq. (9) together with (15)–(18) whereas Table 1 gathers the resulting diameters d, the effective volume fractions, and the resulting $S(0)$. For all concentrations a good fit of the integrated structure factor can be achieved with an effective diameter decreasing slightly with concentration. This is expected in the frame of a perturbative approach.

The small residual deviation of theory and experiment could be removed by relaxing the strict relation of $S(0)$ and the coefficients α to γ. Table 1 gives the $S(0)$ values resulting from such a fit which are only slightly higher than the figures obtained from the fit of the effective diameter. Thus, for the present system $S(0)$ can be determined from the experimental data in good accuracy without resorting to a particular model of interaction.

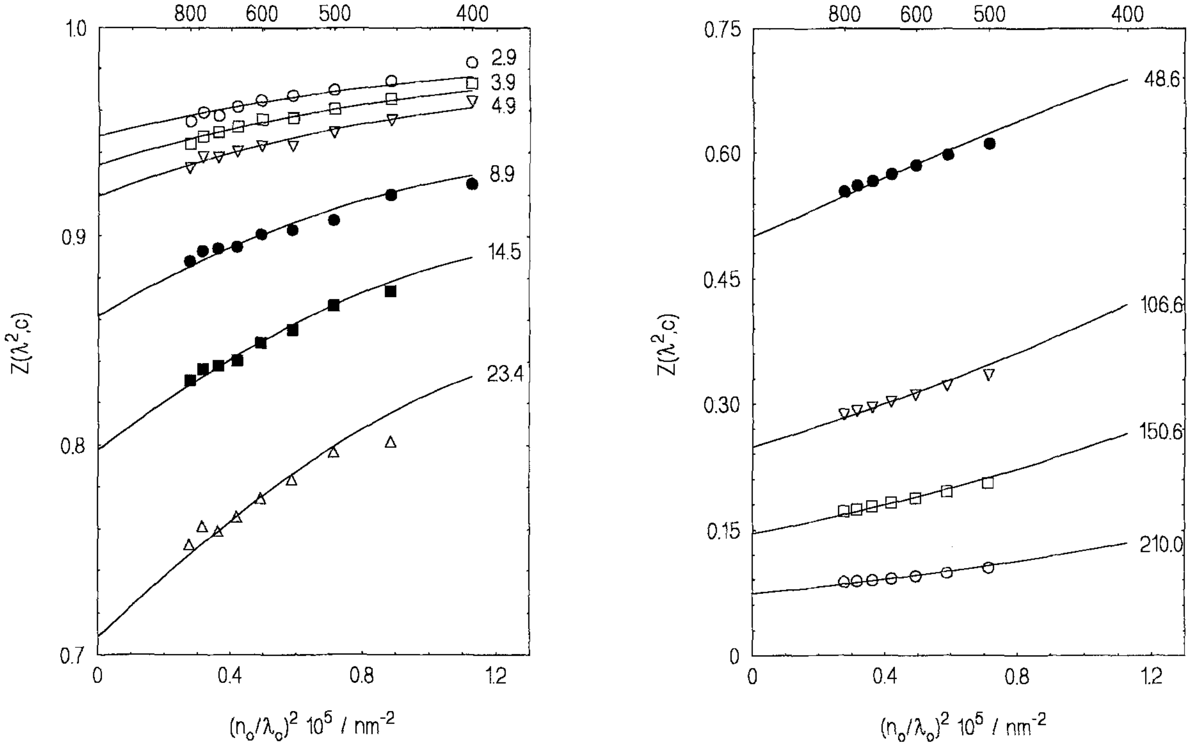

Fig. 5a,b. Integrated structure factor $Z(\lambda^2,c)$ (cf. Eq. (9)) obtained from the experimental turbidities according to Eq. (12). The solid lines show the fit of the theoretical expression Eq. (9) to the experimental data. The resulting fit parameters are gathered in Table 1. The numbers in the graph are the respective concentrations; the figures above the graph indicate the respective wavelength

Table 1. Results of the turbidimetric analysis of the polystyrene latex at different concentrations

$c/(g/l)$	d_{eff}/nm a)	ϕ_{eff} a)	$S(0)$ a)	$S(0)$ b)
2.974	103.6	0.00677	0.947	0.947
3.941	101.7	0.00848	0.935	0.934
4.951	101.09	0.0149	0.920	0.926
8.848	101.11	0.0187	0.861	0.874
14.48	98.69	0.0285	0.797	0.805
23.40	96.82	0.0435	0.708	0.716
48.60	95.91	0.0874	0.500	0.509
106.6	93.38	0.178	0.249	0.258
150.6	92.62	0.245	0.146	0.154
210.00	91.49	0.329	0.0735	0.082

a) Obtained by a fit of the effective diameter to the experimental data of $Z(\lambda^2, c)$ (cf. Eq. (9)) using the Percus-Yevick structure factor (Eq. (15) to (18)).

b) Obtained by a polynomial fit of the experimental data of $Z(\lambda^2, c)$

Again, a thorough comparison of the data given in Table 1 and the parameters obtained from a fit of Eq. (13) to the experimental data has been made despite the finding (see Fig. 2 and the respective discussion) that for the given small standard deviation the influence of polydispersity should be negligible. The analysis of the experimental data corroborates this conclusion since both sets of data agree within 2–3% which is well below experimental uncertainty.

Conclusion

It has been demonstrated that a simple turbidimetric analysis of a polymeric latex is capable of furnishing the structure factor in the region of low q. In particular, the structure factor at $q = 0$ can be obtained in good accuracy. Thus, turbidimetry gives access to highly useful information on particle interaction in a regime of concentration which is difficult to access by other methods.

Acknowledgment

Financial support by the Bayer AG, Geschäftsbereich Kautschuk, and the Bundesministerium für Forschung und Technologie, Pilotprojekt "Mesoskopische Systeme" is gratefully acknowledged. The authors are indebted to H.-G. Müller (Bayer AG) for determining the size distribution of the PS-latex by ultracentrifugation. Y.S. Kim is thanked for the synthesis and the characterization of the polystyrene latex and W. Arbogast for skillful assistance.

References

1. Hunter RJ (1991) Foundations of Colloid Science, Vol 1. Clarendon Press, Oxford
2. Hunter RJ (1991) Foundations of Colloid Science, Vol 2. Clarendon Press, Oxford
3. Candau F, Ottewill RH (1990) An Introduction to Polymer Colloids. Kluwer Academic Publishers Dordrecht
4. Ottewill RH (1990) Faraday Disc Chem Soc 90:1 and further references given there
5. Goodwin JW, Ottewill RH, Owens SM, Richardson RA, Hayer JB (1985) Makromol Chem Suppl 10/11:499
6. Duits MGH, May RP, Vrij A, de Kruif CG (1991) Langmuir 7:62
7. Ashdown S, Markovic I, Ottewill RH, Lindner P, Oberthür RC, Rennie AR (1990) Langmuir 6:303
8. Moonen J, de Kruif C, Vrij A (1988) Colloid Polym Sci 266:1068
9. Moonen J, Vrij A (1988) Colloid Polym Sci 266:1140
10. Duits GH, de Kruif CG, Vrij A (1992) Colloid Polym Sci 270:154
11. Ottewill RH, Richardson RA (1982) Colloid Polym Sci 260:708
12. Härtl W, Segschneider C, Versmold H (1991) Mol Phys 73:541
13. Härtl W, Versmold H, Zhang-Heider X (1991) Ber Bunsenges Phys Chem 95:1105; Härtl W, Versmold H, Linse P (1992) J Phys Chem 97:7797
14. van Helden AK, Vrij A (1980) J Colloid Int Sci 78:312
15. Livsey I, Ottewill RH (1989) Colloid Polym Sci 267:421
16. Kerker M (1969) The Scattering of Light and Other Electromagnetic Radiation. Academic Press, New York
17. Lange H (1968) Colloid Polym Sci 223:24
18. Debye P, Woermann D, Chu B (1962) J Chem Phys 36:851
19. see e.g.: Shen W, Smith GR, Knobler CM, Scott RL (1991) 95:3376 DaMore LW, Jacobs DT (1992) J Chem Phys 97:464; Jayalakshmi Y, Beysens D (1992) Phys Rev Lett A45, 8709 and further literature cited therein
20. Jansen JW, de Kruif CG, Vrij (1986) J Colloid Interf Sci 114:492
21. Rouw W, Vrij A, de Kruif CG (1988) Colloids Surf 31:299
22. Penders MGHM, Vrij A (1990) J Chem Phys 93:3704
23. Grunder R, Kim YS, Ballauff M, Kranz D, Müller HG (1991) Angew Chem Int Ed 30:1650; Grunder R, Urban G, Ballauff M (1992) Colloid Polym Sci (in press)
24. D'Aguanno B, Klein R (1991) J Chem Soc Faraday Trans 87:379
25. Pusey PN, Fijnaut HM, Vrij A (1982) J Chem Phys 77:4270
26. Härtl W, Versmold H (1984) 80:1387
27. Ashcroft NW, Lekner J (1966) Phys Rev 145:145
28. Hansen JP, McDonald IR (1986) Theory of Simple Liquids. Second Edition, Academic Press, London
29. Vrij A (1979) J Chem Phys 77:3267
30. Evans R, Sluckin TJ (1981) J Phys C 14:2569
31. Grimson MJ (1982) J Chem Soc Faraday 2 79:817
32. Maron SH, Pierce PE, Ulevich N (1963) J Colloid Sci 18:470
33. Goodwin JW, Ottewill RH, Parentich A (1990) Colloid Polym Sci 268: 1131
34. Devon MJ, Rudin A (1987) J Appl Polym Sci 34:469; third entry of table I
35. Nieuwenhuis EA, Pathmamanoharan C, Vrij A (1981) J Colloid Interf Sci 81:196
36. Andersen HC, Weeks JD, Chandler D (1971) Phys Rev A4:1597
37. Hayter JB, Penfold J (1981) Mol Phys 42:109
38. Hansen JP, Hayter JB (1982) Mol Phys 46:651
39. Härtl W, Vermold H, Wittig U (1992) Langmuir 8, 2885

Received April 19, 1993;
accepted September 14, 1993

Authors' address:

Prof. Dr. M. Ballauff
Polymer-Institut
Universität (T.H.) Karlsruhe
Kaiserstraße 12
76128 Karlsruhe, FRG